MOLECULAR AND CELLULAR BIOLOGY, Feb. 1999, p. 1427–1437 Vol. 19, No. 2
0270-7306/99/$04.00+0


# Regulation of Ribosomal S6 Protein Kinase-p90$^{rsk}$, Glycogen Synthase Kinase 3, and β-Catenin in Early *Xenopus* Development

MONICA A. TORRES,[1]† HAGIT ELDAR-FINKELMAN,[2] EDWIN G. KREBS,[1,2] AND RANDALL T. MOON[1]*

*Howard Hughes Medical Institute and Department of Pharmacology[1] and Department of Biochemistry,[2] University of Washington School of Medicine, Seattle, Washington*

Received 23 April 1998/Returned for modification 28 May 1998/Accepted 23 October 1998

**β-Catenin is a multifunctional protein that binds cadherins at the plasma membrane, HMG box transcription factors in the nucleus, and several cytoplasmic proteins that are involved in regulating its stability. In developing embryos and in some human cancers, the accumulation of β-catenin in the cytoplasm and subsequently the nuclei of cells may be regulated by the Wnt-1 signaling cascade and by glycogen synthase kinase 3 (GSK-3). This has increased interest in regulators of both GSK-3 and β-catenin. Searching for kinase activities able to phosphorylate the conserved, inhibitory-regulatory GSK-3 residue serine 9, we found p90$^{rsk}$ to be a potential upstream regulator of GSK-3. Overexpression of p90$^{rsk}$ in *Xenopus* embryos leads to increased steady-state levels of total β-catenin but not of the free soluble protein. Instead, p90$^{rsk}$ overexpression increases the levels of β-catenin in a cell fraction containing membrane-associated cadherins. Consistent with the lack of elevation of free β-catenin levels, ectopic p90$^{rsk}$ was unable to rescue dorsal cell fate in embryos ventralized by UV irradiation. We show that p90$^{rsk}$ is a downstream target of fibroblast growth factor (FGF) signaling during early *Xenopus* development, since ectopic FGF signaling activates both endogenous and overexpressed p90$^{rsk}$. Moreover, overexpression of a dominant negative FGF receptor, which blocks endogenous FGF signaling, leads to decreased p90$^{rsk}$ kinase activity. Finally, we report that FGF inhibits endogenous GSK-3 activity in *Xenopus* embryos. We hypothesize that FGF and p90$^{rsk}$ play heretofore unsuspected roles in modulating GSK-3 and β-catenin.**

Analysis of signal transduction cascades has provided key insights into cellular control mechanisms in both adults and embryos. Considerable research has focused on the Wnt signaling pathway since Wnts have been implicated in controlling axis formation in vertebrates; limb polarity, proliferation, and cell fate in the mesoderm and the nervous system; organogenesis; and probably some human cancers (reviewed in reference 6). The best-characterized Wnt signaling pathway, that of Wnt-1 (reviewed in reference 6), works through a Frizzled-related receptor to activate the function of the phosphoprotein Dishevelled, which promotes the inhibition of glycogen synthase kinase 3 (GSK-3). The inhibition of GSK-3 allows the stabilization and accumulation of β-catenin in the cytoplasm (70, 74), which then translocates to the nucleus (21, 42, 74), where it modulates target gene transcription and cell fate by interacting with HMG-box transcription factors (reviewed in references 6, 40, and 45). GSK-3 has been proposed to target β-catenin for degradation by a ubiquitination and proteosome pathway by phosphorylating evolutionarily conserved serine/threonine residues in its N terminus (1, 33, 50, 74). Besides its function in the Wnt signaling pathway, β-catenin is a component of the adherens junction linking cadherins to the cytoskeleton (37).

* Corresponding author. Mailing address: Howard Hughes Medical Institute, Campus Box 357370, University of Washington School of Medicine, Seattle, WA 98195. Phone: (206) 543-1722. Fax: (206) 616-4230. E-mail: rtmoon@u.washington.edu.

† Present address: Department of Molecular and Cellular Physiology, Beckman Center for Molecular and Genetic Medicine, Stanford University School of Medicine, Stanford, CA 94305-5426.

During the early cleavage stages of embryonic development, β-catenin accumulates in the cytoplasm and in the nucleus of the blastomeres on the prospective dorsal side of *Xenopus* embryos (42). This asymmetric accumulation of β-catenin has been hypothesized to be mediated by an inhibition of GSK-3 activity on the future dorsal regions of the embryo (12, 30, 42, 52). Both β-catenin and GSK-3 are required maternal components of the signaling pathway that leads to the specification of dorsal cell fate and the development of the endogenous axis (reviewed in reference 45). Although overexpression of a subset of Wnt proteins in cleavage-stage *Xenopus* embryos leads to a dorsalized phenotype (13, 67) and ectopic Wnt/Wingless signaling inhibits GSK-3 activity (8), causing the accumulation of free β-catenin (31, 42, 51, 70, 74), loss-of-function experiments argue against a requirement for Wnts in the establishment of the endogenous dorsal axis in *Xenopus* (32, 67). This raises the possibility of unsuspected regulators of GSK-3 during *Xenopus* embryogenesis.

Recently, mutant forms of β-catenin that display increased stability and signaling during development (74) have been identified in colon cancer (47) and melanoma (57) cells, making β-catenin a putative oncogene. β-Catenin associates with the protein product of adenomatous polyposis coli (APC), a tumor suppressor gene frequently mutated in colon carcinoma cells (27, 53, 55, 65). APC plays a role in downregulating the levels of free β-catenin in cultured cells (49), although there are conflicting data about whether APC plays a positive or negative role downstream of Wnt signaling during embryogenesis (29, 54, 71). GSK-3, β-catenin, and APC form protein complexes, and GSK-3 is able to phosphorylate APC fragments in vitro (56) and β-catenin in vitro and probably in vivo (74), making both β-catenin and APC putative targets of

GSK-3 in vivo. This process probably involves the additional protein, Axin, which may form a complex with at least GSK-3 and β-catenin (33, 59). These studies suggest that regulation of β-catenin signaling by GSK-3 is relevant during early embryogenesis and adult tumor formation.

Unlike many kinases, GSK-3 is constitutively active in resting cells and undergoes rapid inhibition by growth factors and hormones. Several kinases regulate GSK-3 activity in intact cells. The regulation of GSK-3 activity by insulin probably occurs via activation of phosphatidylinositol-3 (PI-3) kinase and its target of activation, protein kinase B (PKB) (11, 48). Suppression of GSK-3 activity is achieved by phosphorylation of serine 9, located at the amino terminus of the enzyme (11). Mutation of this residue leads to increased, deregulated GSK-3 activity and the consequent inhibition of glycogen synthesis (15). On the other hand, epidermal growth factor inhibits GSK-3 via activation of mitogen-activated protein (MAP) kinase and p90$^{rsk}$ (14, 62), with the latter being capable of phosphorylating GSK-3 at serine 9 (66). With regard to PKC, phorbol esters inhibit GSK-3 activity in cultured cells (62) and PKC regulates GSK-3 activity in vitro (23). Moreover, using inhibitors for PKC, Cook et al. (8) have suggested that inhibition of GSK-3 by Wnt/Wingless signaling may be mediated by PKC. Finally, β-adrenergic agonists also inhibit GSK-3 activity in cultured cells (48).

In this study, we searched for kinases that may potentially function upstream of GSK-3 in *Xenopus* eggs, by screening for kinases capable of phosphorylating the regulatory-inhibitory site, serine 9, of GSK-3 (15, 58, 62, 66). We found that p90$^{rsk}$ may function as an upstream regulator of GSK-3 and we show that both endogenous p90$^{rsk}$ and GSK-3 are downstream targets of FGF, regulated in a reciprocal manner, in early *Xenopus* development. Overexpression of p90$^{rsk}$ was found to have no effect on steady-state levels of free β-catenin or on dorsal-axis formation but, instead, promotes the accumulation of β-catenin at the plasma membrane when overexpressed in the marginal zone of *Xenopus* embryos. Finally, we demonstrate for the first time that fibroblast growth factor (FGF) signaling leads to the inhibition of endogenous GSK-3 activity. These data support a role for p90$^{rsk}$ in FGF-mediated processes, such as mesoderm and neural induction and patterning, and demonstrate that the GSK-3 and β-catenin are targets of the FGF/p90$^{rsk}$ signaling pathway during early *Xenopus* development.

## MATERIALS AND METHODS

**cDNA constructs and embryo microinjection.** *XS6KIIA* (generated by PCR from the published sequence) (35), *N/C XS6KIIA* (generated by PCR substitution, with lysines 94 and 445 changed to arginines) and a nonfunctional *XS6KIIA* (containing a nonsense mutation) were subcloned into the $CS2^+$ expression vector (a gift of D. Turner and R. Rupp, Fred Hutchinson Cancer Research Center, Seattle, Wash.). All constructs were then fully sequenced to confirm their identity. The genes encoding *Xenopus* embryonic FGF (*eFGF*) (34), *Xenopus* dominant negative FGF receptor (*dnFGFR*) (2), *Xenopus* β-catenin–*myc* (74), β-galactosidase (67), and green fluorescent protein (73) and the above constructs were obtained and transcribed as described previously (67, 74). Embryos were microinjected with these RNAs and cultured as described (67, 74); further details are given in the figure legends. In vitro-translated [$^{35}$S]β-catenin protein was generated using β-catenin–myc DNA (74) as a template for the coupled in vitro transcription-translation TNT coupled reticulocyte lysate systems kit (Promega, Madison, Wis.). mRNA present in the reticulocyte lysates after the transcription-translation reaction was degraded by RNase A treatment followed by RNasin treatment to inhibit RNase A activity.

**Protein extractions and immunoprecipitations.** *Xenopus* eggs or embryos were homogenized (50 per sample) on ice in 300 μl of buffer H (50 mM β-glycerophosphate [pH 7.3], 2 mM EDTA, 2 mM EGTA, 1 mM NaF, 0.3 mM $Na_3VO_4$, 1 mM benzamidine, 25 μg of aprotinin per ml, 25 μg of leupeptin per ml, 1 mM dithiothreitol). To remove yolk proteins, 300 μl of 1,1,2-trichlorotrifluoroethane (Sigma) was added to each sample, which was then vortexed for 30 s. The samples were centrifuged for 10 min at 4°C and 1,000 × *g*, and the supernatant was mixed with Triton X-100 (final concentration, 0.25%) and incubated at 4°C for 10 min with 10 s of vortexing every 2 min. The samples were centrifuged for 30 min at 4°C and 9,000 × *g*. Supernatants were used immediately or stored at −80°C for in-gel kinase reactions and Western blotting or were pooled (to obtain approximately 10 mg of total protein), diluted with buffer H (final Triton X-100 concentration, 0.1%), filtered through glass wool, and subjected to fast protein liquid chromatography (FPLC) Mono-Q fractionation. Fractions were eluted with a linear 0 to 0.25 M NaCl gradient. To determine the spatial distribution of p90$^{rsk}$ kinase activity within a 32-cell *Xenopus* embryo, embryos were dissected into animal and vegetal halves or into dorsal and ventral halves and protein was extracted from 20 halves per sample in buffer H as described above for in-gel kinase assays.

To measure GSK-3 kinase activity, 50 *Xenopus* embryos per sample were homogenized and processed as described above with a modified buffer H (50 mM β-glycerophosphate [pH 7.3], 1 mM EDTA, 1 mM EGTA, 0.1 mM $Na_3VO_4$, 1 mM benzamidine, 25 μg of aprotinin per ml, 25 μg of leupeptin per ml, 1 mM dithiothreitol). The samples were then pooled (to obtain approximately 12 mg of total protein), diluted with modified buffer H (final Triton X-100 concentration, 0.2%), filtered through glass wool to remove lipids, and subjected to FPLC Mono-Q fractionation. The GSK-3 activity in the flowthrough and wash fractions (1 ml of each fraction) was assayed.

Soluble protein was extracted by homogenizing 50 *Xenopus* embryos per sample on ice in 300 μl of buffer H in the absence of detergents, as described above. Then 300 μl of 1,1,2-trichlorotrifluoroethane was added to each sample, and the samples were subjected to 30 s of vortexing to remove yolk proteins. The samples were then centrifuged for 10 min at 12,000 × *g* and 4°C, and the supernatant was stored at −80°C or used immediately for Western blotting.

To study membrane-associated β-catenin, 50 *Xenopus* embryos per sample were homogenized on ice in 400 μl of RIPA buffer (50 mM HEPES [pH 7.4], 150 mM NaCl, 2 mM EDTA, 1% Triton X-100, 0.5% sodium deoxycholate, 0.1% sodium dodecyl sulfate [SDS], 1 μg of leupeptin per ml) and centrifuged for 10 min at 12,000 × *g* and 4°C. The supernatant fraction was diluted with RIPA buffer and incubated with concanavalin A (ConA)-Sepharose beads (Pharmacia LKB Biotech, Piscataway, N.J.) (50 μl of slurry per 500 μl of sample) for 1 h at 4°C to obtain a cadherin-enriched fraction (19, 46). ConA Sepharose beads with associated β-catenin were washed three times in 1 ml of RIPA buffer and then treated with λ-phosphatase (New England Biolabs) and/or prepared for SDS-polyacrylamide gel electrophoresis (PAGE).

For p90$^{rsk}$ immunoprecipitation experiments, 10 *Xenopus* embryos per sample were homogenized on ice in 300 μl of buffer H with 1% Triton X-100 and centrifuged for 10 min at 12,000 × *g* and 4°C. Then 200 μl of supernatant was incubated for 1 h at 4°C with 5 μl of rabbit anti-p90$^{rsk}$ antibody (14) and 20 μl of protein A-Sepharose 4B Fast Flow beads (Sigma) in a final volume of 500 μl. The beads were washed twice with 0.5 M LiCl in 50 mM Tris-Cl (pH 7.5) and twice in 50 mM Tris-Cl (pH 7.5). The samples were used immediately in S6 peptide kinase reactions. Alternatively, the same immunoprecipitation procedure was used to deplete p90$^{rsk}$ from protein extracts of unfertilized *Xenopus* eggs and of 2-cell, 32-cell, and 128-cell embryos (50 per sample) used for the in-gel kinase reactions.

**Kinase and phosphatase reactions.** For in-gel kinase reactions, protein extracts equivalent to five embryos mixed with SDS loading buffer (final concentration, 2% SDS and 2.5% β-mercaptoethanol) were loaded without boiling onto 10% mini-polyacrylamide gels (29:1 acrylamide/bisacrylamide ratio) polymerized with or without 1 mg of Crosstide peptide (GRPRTSSFAEG) (11) per ml and subjected to SDS-PAGE. The gels were then washed twice in 50 mM Tris-Cl (pH 8.0) and 20% 2-propanol for 30 min, once in buffer A (50 mM Tris-Cl [pH 8.0], 5 mM β-mercaptoethanol) for 1 h, and twice in buffer A with 6 M guanidine HCl for 30 min, all at room temperature (RT). The gels were washed for 16 to 24 h at 4°C in buffer A with 0.04% Tween 40, with at least five changes of buffer. The in-gel phosphorylation reaction was then carried out by incubating the gels in reaction mix (40 mM HEPES [pH 8.0], 25 μM cold ATP, 2 mM dithiothreitol, 100 μM EGTA, 5 mM $MgCl_2$, 250 μCi of [γ-$^{32}$P]ATP [3,000 Ci/mmol]) for 1 h at RT with vigorous shaking. The gels were washed with 5% trichloroacetic acid and 1% sodium pyrophosphate at RT to reduce background radioactivity, dried, and exposed to an autoradiograph with an intensified at −70°C. This procedure was modified from published experiments (24, 36).

In-solution Crosstide kinase reactions were performed by mixing a 12-μl FPLC Mono-Q fraction aliquot from oocyte protein extracts with 15 μl of kinase reaction buffer containing 25 mM β-glycerophosphate (pH 7.3), 0.5 mM dithiothreitol, 1 mM EGTA, 0.1 mM orthovanadate, 100 mM $MgCl_2$, 0.1 mg of bovine serum albumin per ml, 100 μM Crosstide peptide, and 100 μM [γ-$^{32}$P]ATP (0.25 mCi/mmol). The kinase reaction mixtures were incubated for 15 min at 30°C, spotted on p81 paper, and counted for radioactivity.

For S6 peptide kinase reactions, p90$^{rsk}$ was immunoprecipitated from embryo extracts and then incubated with kinase reaction mix, [γ-$^{32}$P]ATP, and S6 peptide substrate as described previously (14). Then 25 μl of the kinase reaction mixture was spotted on p81 phosphocellulose paper after 15 min of incubation at 30°C, and the paper was processed as described above.

GSK-3 activity was assayed in FPLC Mono-Q fractions from embryo extracts with a synthetic phosphopeptide, p9CREB [ILSRRPS(p)YR], substrate. Aliquots (12 μl) from each fraction were mixed with 12 μl of reaction buffer (100 μM peptide, 50 μM [γ-$^{32}$P]ATP [0.25 mCi/ml], 0.01% β-mercaptoethanol, 20

nM microcysteine [Calbiochem]). The reaction mixtures were incubated for 15 min at 30°C and then spotted on p81 paper and counted for radioactivity.

The membrane-associated β-catenin fraction was treated with 800 U of λ-phosphatase (New England Biolabs) by resuspending the ConA-Sepharose beads (see above) in the λ-phosphatase reaction mix as specified by the manufacturer and incubating the mixture for 30 min at 30°C. The beads were then washed in 50 mM Tris-Cl (pH 7.5), resuspended in SDS loading buffer boiled for 10 min, and analyzed by SDS-PAGE with 7.5% minigels (Bio-Rad) and Western blotting.

**Western blotting.** All Western blot analyses were performed with 0.45-μm-pore-size nitrocellulose filters. p90$^{rsk}$ was detected with a primary polyclonal rabbit anti-p90$^{rsk}$ antibody raised against the C terminus of the enzyme (14). Endogenous β-catenin was detected with a primary polyclonal rabbit anti-β-catenin antibody which associates with its N terminus (42, 74). α-Spectrin was detected with a primary rabbit anti-α-spectrin antibody (22). All of these immunoblots were then incubated with a horseradish peroxidase (HRP)-conjugated goat anti-rabbit secondary antiserum (Zymed). Ectopic β-catenin–myc was detected with a primary monoclonal mouse anti-c-*myc* antibody, followed by an HRP-conjugated goat anti-mouse secondary antiserum (74). Endogenous GSK-3 was detected with a primary monoclonal mouse anti-GSK-3 antibody (Transduction Laboratories, Lexington, Ky.). GSK-3 serine 9 phosphorylation was detected with a primary monoclonal mouse anti-GSK-3 phosphoserine 9 antibody (Upstate Biotechnology Inc. and Calbiochem). These primary antibodies were detected with a biotinylated anti-mouse secondary antiserum (Vector, Burlingame, Calif.) and an HRP-conjugated streptavidin (Zymed) incubation. The HRP signal was visualized by a Renaissance Western blot chemilumnescence reagent (NEN Life Science Products, Boston, Mass.). Signals for β-catenin, α-spectrin, and p90$^{rsk}$ were quantitated by densitometry (model UA-5 Absorbance/Fluorescence detector; Isco, Lincoln, Neb.). β-Catenin and p90$^{rsk}$ protein levels were compared after normalization for α-spectrin, to control for variability in protein content. [$^{35}$S]β-catenin was detected with a Storm 820 PhosphorImager and quantitated with ImageQuant (Molecular Dynamics, Sunnyvale, Calif.).

## RESULTS

**p90$^{rsk}$ is a potential inhibitor of GSK-3 during early *Xenopus* embryogenesis.** To identify kinase activities capable of inhibiting GSK-3 activity during early *Xenopus* development, we screened for kinases which are able to phosphorylate GSK-3 residue serine 9. Phosphorylation of this conserved regulatory residue results in the inhibition of GSK-3 activity (58, 62, 66). As our substrate, we used a peptide termed Crosstide, patterned after the N terminus of GSK-3, which includes serine 9 (11). In-gel kinase reactions were performed with protein extracted from unfertilized *Xenopus* eggs and with gels polymerized with and without Crosstide peptide (Fig. 1A). We identified a 90-kDa Crosstide kinase activity (Fig. 1A), which we hypothesized to be *Xenopus* p90$^{rsk}$, based on protein size (35), the fact that it was previously shown to phosphorylate GSK-3 (62, 66), and the fact that *Xenopus* oocytes display high p90$^{rsk}$ kinase activity (16, 17). To test if this Crosstide kinase activity was p90$^{rsk}$, we analyzed the proteins extracted from *Xenopus* unfertilized eggs by FPLC Mono-Q fractionation and found that one of the eluted peaks of Crosstide kinase activity (Fig. 1B) correlated with the peak of p90$^{rsk}$ protein as determined by Western blotting (Fig. 1B, fractions 26 to 36, 0.1 M NaCl gradient). We next performed immunodepletion experiments in which p90$^{rsk}$ was immunoprecipitated from the protein extracts prior to SDS-PAGE followed by in-gel kinase reactions. This procedure resulted in removal of the majority of 90-kDa kinase activity from unfertilized eggs (Fig. 1C, lane 1), as well as from cleavage-stage embryos (lanes 2 to 4). Control immunodepletion experiments performed in the absence of antibody did not deplete the 90-kDa kinase activity (data not shown). These data indicate that it is highly likely that the 90-kDa Crosstide kinase activity (Fig. 1A) detected in the in-gel kinase assays is p90$^{rsk}$ and that p90$^{rsk}$ is a potential upstream regulator of GSK-3 during *Xenopus* embryogenesis.

We next analyzed the spatial distribution of p90$^{rsk}$ kinase activity during the early cleavage stages of *Xenopus* development, at which time β-catenin is more stable on the future dorsal side than on the ventral side of the embryo (42), presumably due to lower GSK-3 activity (12, 30, 52). p90$^{rsk}$ kinase activity was present almost exclusively in the animal hemisphere of the *Xenopus* 32-cell embryo (Fig. 2A, compare lanes 1 and 2), with little reproducible dorsoventral asymmetry (compare lanes 3 and 4). When Western blotting rather than kinase activity was used, it was shown that p90$^{rsk}$ is present in unfertilized *Xenopus* eggs (Fig. 2B, lane 1), in cleavage-stage embryos (lane 2), during mesoderm induction (lane 4), and through the start of gastrulation (lane 5). In unfertilized eggs, p90$^{rsk}$ appears as a doublet, with a subset of protein displaying an electrophoretic mobility shift. This is consistent with p90$^{rsk}$ hyperphosphorylation and activation, as has been reported for p90$^{rsk}$ in *Xenopus* oocytes (16, 17).

**p90$^{rsk}$ overexpression increases total steady-state levels of endogenous β-catenin.** Since inhibition of GSK-3 results in the stabilization of β-catenin (74) and p90$^{rsk}$ may function as a maternal regulator of GSK-3 activity during early *Xenopus* development, we tested whether overexpression of p90$^{rsk}$ would lead to increased total steady-state levels of endogenous β-catenin. Microinjection of 30 ng of *XS6KIIA* mRNA encoding p90$^{rsk}$ into the marginal zone of four-cell embryos led to a statistically significant 215% increase in steady-state levels of endogenous β-catenin relative to controls ($P < 0.01$ by Student's *t* test; $n = 7$, standard error [SE], 24) (Table 1; Fig. 3A, top gel, lanes 2 and 3 relative to control lane 1). This effect was also obtained with 10-fold-lower levels of ectopic p90$^{rsk}$ RNA (Fig. 3A, compare control lane 4 with XS6KIIA-injected lanes 5 and 6). β-Catenin and p90$^{rsk}$ levels were normalized to α-spectrin on the same Western blots to control for protein quality and even loading. In a related experiment, β-catenin was labeled in vitro with [$^{35}$S]methionine and injected into embryos; this was followed by injection of RNAs. Consistent with the effects on endogenous β-catenin, we observed that *XS6KIIA* RNA but not prolactin RNA increased the level of [$^{35}$S]β-catenin approximately twofold, as quantitated by PhosphorImager analysis (data not shown). Lastly, microinjection of *XS6KIIA* mRNA into the animal pole of two-cell embryos did not increase total endogenous β-catenin levels (87% of control levels, $n = 6$; Table 1), suggesting that responsiveness to p90$^{rsk}$ signaling is not equivalent in all regions of the developing *Xenopus* embryo.

We predicted that the observed increase in steady-state levels of endogenous β-catenin would be dependent on the kinase activity of p90$^{rsk}$ rather than on an unsuspected activity. To test this hypothesis, we microinjected *N/C XS6KIIA* mRNA into the marginal zone of four-cell embryos (Fig. 3B; Table 1). *N/C XS6KIIA* encodes a mutant, putative kinase-dead N/C p90$^{rsk}$ with conserved lysines 94 and 445 in the ATP-binding domain of both N-terminal and C-terminal catalytic domains (4, 20, 35) changed to arginines by PCR substitution. Overexpression of N/C p90$^{rsk}$ did not raise total steady-state levels of endogenous β-catenin (92% of control levels, $n = 4$; Fig. 3B, top gel, compare control lane 1 with injected lanes 2 and 3; Table 1), even when N/C p90$^{rsk}$ was overexpressed at high levels (Fig. 3B, bottom gel, compare control lane 1 with injected lanes 2 and 3; Table 1). This result demonstrates that the kinase activity of p90$^{rsk}$ kinase is required to increase total endogenous β-catenin levels in *Xenopus* embryos. Demonstrating that not all kinases increase β-catenin levels, we found that overexpression of a constitutively active form of PKB (a gift of Richard Roth, Stanford University) did not elevate endogenous β-catenin levels (data not shown).

Since differences in β-catenin accumulation are more readily monitored by observing newly synthesized ectopic β-catenin, β-catenin was tagged with a c-*myc* epitope to distinguish it from the large amount of endogenous β-catenin, which is prob-

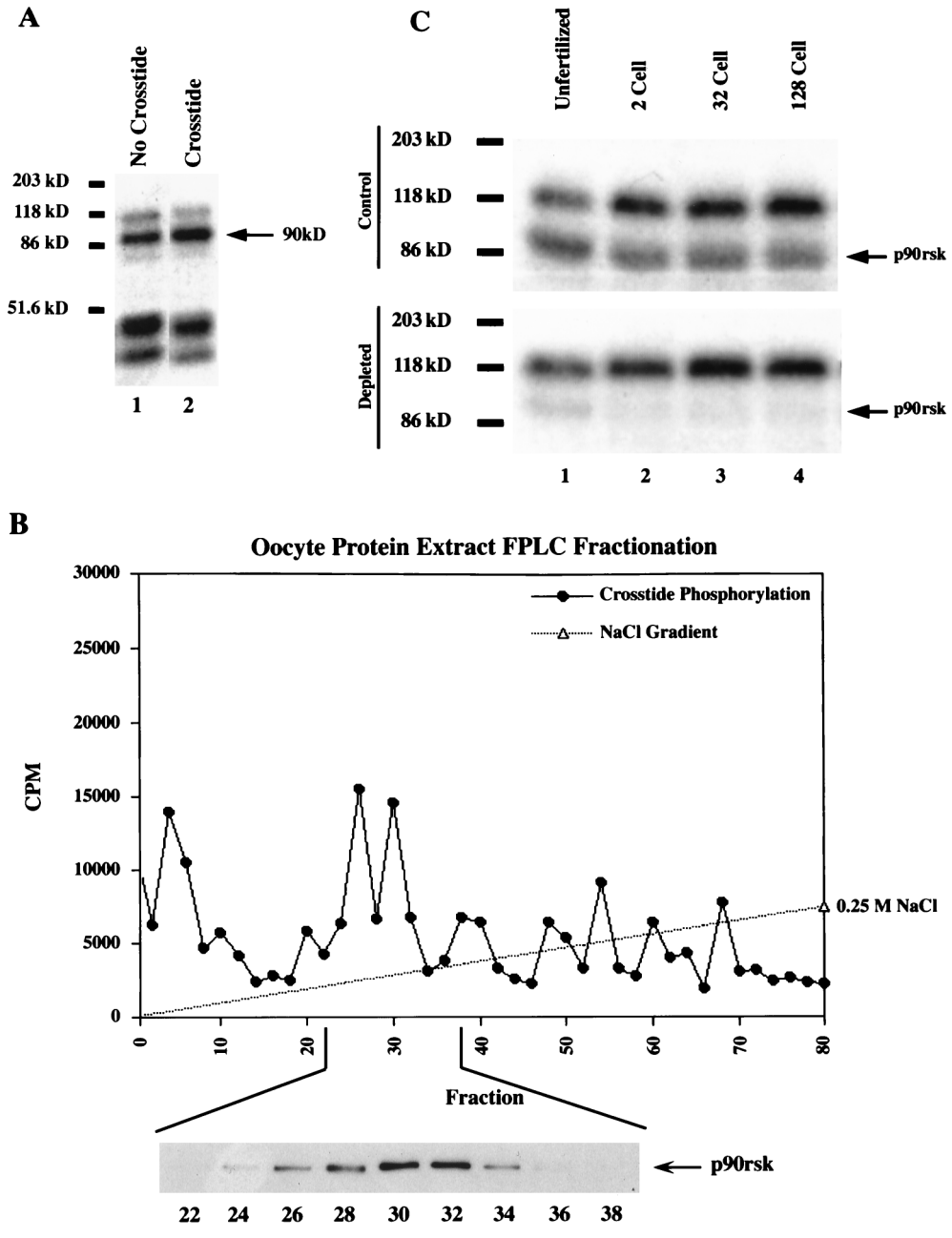


FIG. 1. p90$^{rsk}$ kinase activity is present in unfertilized *Xenopus* eggs. (A) Assays for p90$^{rsk}$ activity were carried out in extracts from unfertilized *Xenopus* eggs by using an in-gel kinase assay as described in Materials and Methods. In the absence of an exogenous substrate (Crosstide), several phosphorylated proteins were seen in the egg protein extract (lane 1). In the presence of Crosstide, a 90-kDa kinase activity is increased, indicating specific phosphorylation of the exogenous substrate (lane 2). (B) The possibility that the 90-kDa kinase activity is p90$^{rsk}$ was tested by using FPLC Mono-Q fractionation followed by Crosstide kinase assays and Western blot analysis. A peak of Crosstide kinase activity was eluted at approximately 0.1 M NaCl in fractions 24 to 36. Western blot analysis confirmed the presence of p90$^{rsk}$ kinase in these fractions (inset). The majority of Crosstide kinase activity was present in the flowthrough (data not shown), including fractions 1 to 10 as the shoulder of this activity; however, p90$^{rsk}$ was not present in the flowthrough fractions. (C) In-gel kinase assays performed without an exogenous substrate reveal a 90-kDa kinase activity present in unfertilized egg and in 2-, 32-, and 128-cell embryo extracts (lanes 1 to 4, top gel). Immunodepletion of p90$^{rsk}$ kinase from these protein extracts with an anti-p90$^{rsk}$ polyclonal antibody prior to the in-gel kinase assays results in the removal of the 90-kDa band (bottom gel), demonstrating that the 90-kDa kinase activity band is p90$^{rsk}$.

ably rather stable at the plasma membrane (42, 74). We then tested whether overexpression of p90$^{rsk}$ would lead to the accumulation of β-catenin–myc (Fig. 4). As with endogenous β-catenin, ectopic p90$^{rsk}$ but not N/C p90$^{rsk}$ increased total steady-state levels of ectopic β-catenin–myc after normalization of α-spectrin levels (Fig. 4, compare *XS6KIIA* lane 4 with control lane 2 and *N/C XS6KIIA* lane 3).

Previous studies have reported that replacement of the conserved lysine with arginine in the ATP-binding region of the N-terminal, protein kinase A-like catalytic domain leads to a dominant negative form of p90$^{rsk}$ (4). We coexpressed p90$^{rsk}$ along with N/C p90$^{rsk}$ to determine whether the mutant, putative kinase-dead form was capable of antagonizing the effects of ectopic wild-type p90$^{rsk}$. N/C p90$^{rsk}$ inhibited β-catenin–myc

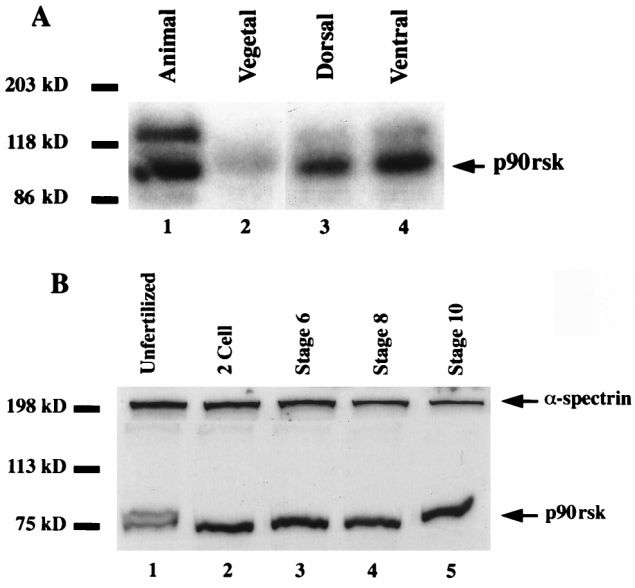


FIG. 2. p90$^{rsk}$ kinase is present in *Xenopus* embryos. (A) Microdissection of 32-cell embryos into animal and vegetal or into dorsal and ventral halves followed by in-gel kinase assays reveals that p90$^{rsk}$ activity is present almost exclusively in the animal hemisphere of *Xenopus* embryos (compare lanes 1 and 2). The dorsal and ventral halves appear to possess approximately equivalent amounts of p90$^{rsk}$ activity (lanes 3 and 4, respectively). (B) Western blot analysis demonstrates that p90$^{rsk}$ protein is present in unfertilized *Xenopus* eggs and in *Xenopus* embryos at various early stages of development (lanes 1 to 5). To control for protein extract quality and gel loading, α-spectrin Western blots were performed with the same nitrocellulose filter (top of gel). In unfertilized egg extracts, a portion of the p90$^{rsk}$ displays an electrophoretic mobility shift, consistent with p90$^{rsk}$ hyperphosphorylation and/or activation (lane 1).

accumulation only at a 2:1 ratio of mutant to wild-type p90$^{rsk}$ (Fig. 4, compare *XS6KIIA* lane 4 with coinjected lanes 5 and 6). We also tested whether N/C p90$^{rsk}$ was capable of inhibiting the kinase activity of ectopically expressed wild-type p90$^{rsk}$. Microinjection of a 1:1 ratio of *XS6KIIA* and *N/C XS6KIIA* RNAs followed by immunoprecipitation of p90$^{rsk}$ and kinase activity assays with S6 peptide as a substrate revealed that ectopic N/C p90$^{rsk}$ partially inhibits the *XS6KIIA*-mediated increase in S6 peptide phosphorylation from a 4-fold stimulation above controls with ectopic p90$^{rsk}$ alone (see Fig. 6A, $P < 0.01$ by Student's $t$ test, $n = 8$) to a 1.5-fold stimulation in the presence of ectopic p90$^{rsk}$ and N/C p90$^{rsk}$ (see Fig. 6A, $P < 0.05$ by Student's $t$ test, $n = 3$). Taken together, these data suggest that in *Xenopus* embryos, N/C p90$^{rsk}$ behaves as a competitive antagonist and not in a dominant negative manner.

**p90$^{rsk}$ overexpression increases the steady-state levels of membrane-associated but not free β-catenin.** To determine whether the p90$^{rsk}$-mediated increase in steady-state β-catenin levels was due to an accumulation of free or complexed protein, we generated a cadherin-enriched membrane fraction by using ConA-Sepharose beads that bind cadherins (19, 46) and a cytoplasmic fraction by omitting detergents from the protein extraction. Overexpression of p90$^{rsk}$ increased the amount of endogenous membrane-associated β-catenin, but this was evident only after λ-phosphatase treatment (Fig. 5A, compare control lanes 4 and 5 with *XS6KIIA* lane 6). This result suggests that phosphorylation may mask the N-terminal β-catenin epitope detected by the polyclonal anti-β-catenin antibody used in Western blotting. Accumulation of newly synthesized, ectopic β-catenin–myc in the membrane fraction was detected with the C-terminal anti-c-*myc* monoclonal antibody (Fig. 5A, bottom gel, compare *XS6KIIA* lanes 3 and 6 with control lanes 2 and 5, respectively) before and after λ-phosphatase treatment (Fig. 5A, compare lanes 2 and 3 with lanes 5 and 6). Only trace amounts of β-catenin and β-catenin–myc were detectable by enhanced chemiluminescence in the supernatant fractions after ConA enrichment (data not shown). Overexpressed p90$^{rsk}$ also increased the levels of injected [$^{35}$S]β-catenin in the cadherin-enriched ConA pellet fraction but not the supernatant fraction (Fig. 5C, detected by PhosphorImager analysis). These data confirm that p90$^{rsk}$ overexpression leads to increased levels of membrane-associated β-catenin and suggests that p90$^{rsk}$ mediates the phosphorylation of the N terminus of β-catenin in a direct or indirect manner. The p90$^{rsk}$-mediated increase in membrane association of endogenous and myc-tagged ectopic β-catenin levels is very similar to that observed for steady-state levels of total β-catenin in the corresponding experiments in Fig. 3A. This suggests that p90$^{rsk}$ increases total β-catenin levels by promoting its association with the membrane. However, due to the ConA enrichment protocol, which rules out normalization of β-catenin levels to α-spectrin as in Fig. 3A, it is not possible to compare these experiments in a quantitative manner.

To examine the steady-state levels of free, cytoplasmic β-catenin, we extracted protein in the absence of detergents. In contrast to the effects of activation of the Wnt signaling pathway (42, 74), we found that p90$^{rsk}$ overexpression did not raise the steady-state level of free endogenous β-catenin (Fig. 5B, top gel compare control lanes 1 and 2 with *XS6KIIA* lane 3) or of free ectopic β-catenin–myc (Fig. 5B, bottom gel, compare control lane 2 with *XS6KIIA* lane 3). Duplicate samples treated with λ-phosphatase were identical to those shown in Fig. 5B (data not shown). Consistent with this result, we were unable to rescue the dorsal cell fate in embryos ventralized by UV irradiation (Table 2), a phenotype which can be rescued by increasing free β-catenin levels (42, 74). Overexpression of p90$^{rsk}$ in control, untreated embryos also failed to alter the dorsoventral fate and instead caused gastrulation defects in 67% (30 ng of RNA, $n = 51$) and 22% (3 ng of RNA, $n = 90$) of the embryos when *XS6KIIA* mRNA was microinjected into the dorsal marginal zone of four-cell embryos. This phenotype was not observed with microinjection of the same doses of *N/C XS6KIIA* mRNA (data not shown).

**FGF signaling stimulates p90$^{rsk}$ and inhibits endogenous GSK-3 kinase activity during early *Xenopus* development.** We

TABLE 1. Steady-state levels of endogenous β-catenin after *XS6KIIA* mRNA microinjection[a]

| mRNA[a] | β-Catenin level (%) | $P$ | SE | $n$ | p90$^{rsk}$ level (%) | $n$ |
|---|---|---|---|---|---|---|
| Control AP | 100 | | | 6 | 100 | 2 |
| *XS6KIIA* AP | 87 | <0.5 | 29 | 6 | 300–2,733 | 2 |
| Control MZ | 100 | | | 7 | 100 | 6 |
| *XS6KIIA* MZ | 215 | <0.01 | 24 | 7 | 1,567 | 6 |
| Control | 100 | | | 5 | 100 | 4 |
| *N/C XS6KIIA* MZ | 92 | <0.005 | 2 | 4 | 419 | 4 |

[a] *XS6KIIA* (1.5 or 15 ng) and *N/C XS6KIIA* (2.5 or 3.75 ng) mRNAs were microinjected twice into the marginal zone (MZ) of four-cell embryos. Alternatively, *XS6KIIA* mRNA (1.5 and 15 ng) was microinjected twice into the animal pole (AP) of two-cell embryos. Only microinjection of *XS6KIIA* mRNA into the marginal zone led to increased steady-state levels of endogenous β-catenin relative to controls (215%, $n = 7$, SE = 24, high and low doses), with an average of 15-fold more p90$^{rsk}$ being expressed in these experiments. In all cases, high- and low-dose RNA injections had identical effects on β-catenin levels. Western blotting and densitometry were used to detect and quantitate β-catenin and p90$^{rsk}$ protein levels.

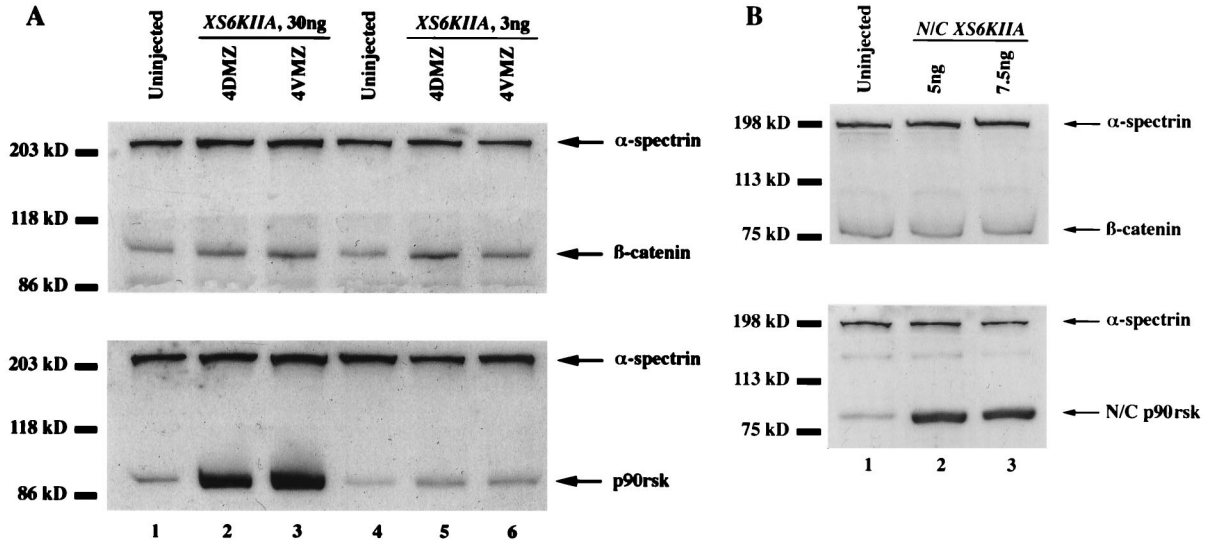


FIG. 3. Overexpression of p90$^{rsk}$ leads to increased steady-state levels of endogenous β-catenin. (A) *XS6KIIA* mRNA (total of 30 or 3 ng) encoding *Xenopus* p90$^{rsk}$ kinase was microinjected into the marginal zone of both dorsal or ventral blastomeres at the four-cell stage (4DMZ and 4VMZ, respectively). Total β-catenin and p90$^{rsk}$ steady-state levels were determined by Western blot analysis. Small elevations in p90$^{rsk}$ protein levels are sufficient to increase the steady-state levels of endogenous β-catenin (compare control lane 4 with *XS6KIIA*-injected lanes 5 and 6). α-Spectrin Western blot analyses were performed with the same nitrocellulose filter to control for protein extract quality and gel loading. After normalization to α-spectrin levels, microinjection of *XS6KIIA* mRNA (3 or 30 ng) into the dorsal or ventral marginal zones of *Xenopus* embryos leads to a statistically significant 215% increase in total endogenous β-catenin steady-state levels relative to untreated controls ($n = 7$, $P < 0.01$ by Student's $t$ test, SE, 24; compare control lanes 1 and 4 to *XS6KIIA*-injected lanes 2 and 3 or 5 and 6). Experiments with either 30 or 3 ng of injected *XS6KIIA* RNA yielded identical results. (B) *N/C XS6KIIA* mRNA (2.5 and 3.5 ng) encoding a mutant, putative kinase-dead N/C p90$^{rsk}$ with conserved ATP-binding domain lysines 94 and 445 changed to arginines was microinjected into the marginal zone of both dorsal or ventral blastomeres at the four-cell stage (ventral microinjection experiment shown). Overexpression of N/C p90$^{rsk}$ does not increase total steady-state levels of endogenous β-catenin (compare control lane 1 to N/C XS6KIIA-injected lanes 2 and 3), with average β-catenin levels of 92% ($n = 4$) relative to controls, after normalization to α-spectrin signal on the same Western blot.

hypothesized that p90$^{rsk}$ kinase is activated by endogenous FGF, since the FGF signaling pathway is active during mesoderm induction in early *Xenopus* development (3, 38) and stimulates the MAP kinase pathway during mesoderm induction (25, 28, 69) and since previous studies have shown that p90$^{rsk}$ is a downstream target of MAP kinase (18, 63, 64). Ectopic eFGF increased endogenous p90$^{rsk}$ kinase activity to 200% of control levels (Fig. 6A, $n = 2$), and microinjection of *XS6KIIA* RNA led to a fourfold increase in p90$^{rsk}$ kinase activity above controls, as measured by S6 peptide kinase assays (Fig. 6A, $P < 0.01$ by Student's $t$ test, $n = 8$). We found that overexpression of p90$^{rsk}$ along with eFGF led to a synergistic, 170-fold increase in p90$^{rsk}$ kinase activity above control levels (Fig. 6A, $P < 0.005$ by Student's $t$ test; $n = 4$). Conversely, overexpression of a dnFGFR, which inhibits endogenous FGF signaling (2), inhibited p90$^{rsk}$ activation from 414% above controls to 166% (Fig. 6A, $P < 0.05$ by Student's $t$ test, $n = 4$). Microinjection of eFGF RNA (4 ng) but not prolactin RNA (4 ng) also stimulated a 90-kDa Crosstide kinase activity, which comigrated with p90$^{rsk}$ activity in our in-gel kinase assays (Fig. 6B, $n = 2$). These data suggest that FGF is an upstream activator of p90$^{rsk}$. In support of this hypothesis, eFGF overexpression in *Xenopus* embryos mimics p90$^{rsk}$ overexpression by increasing the association of endogenous β-catenin with the

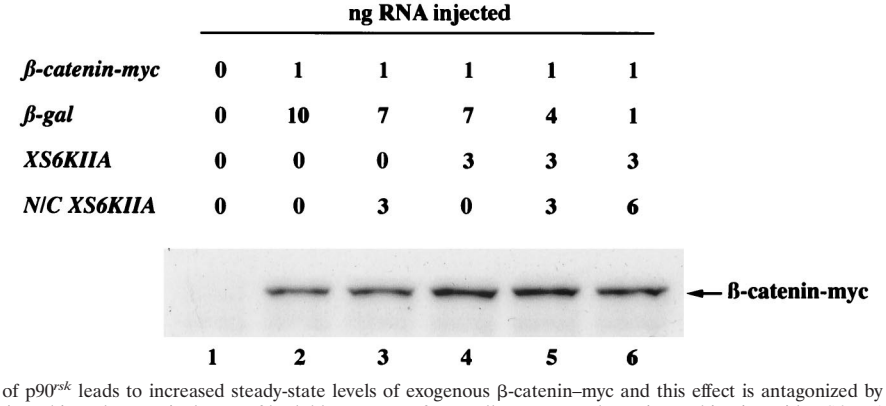


FIG. 4. Overexpression of p90$^{rsk}$ leads to increased steady-state levels of exogenous β-catenin–myc and this effect is antagonized by N/C p90$^{rsk}$. β-Catenin–*myc* mRNA (0.5 ng) was microinjected into the marginal zone of both blastomeres of two-cell *Xenopus* embryos in combination with *XS6KIIA* (3 ng) and/or *N/C XS6KIIA* (1.5 or 3 ng) mRNA, which encode p90$^{rsk}$ and putative kinase-dead N/C p90$^{rsk}$, respectively. Control β-galactosidase (β-gal) mRNA was added to the mRNA mix to keep the total amount of mRNA microinjected constant (11 ng). Microinjection of *XS6KIIA* (lane 4) but not *N/C XS6KIIA* (lane 3) mRNA leads to the increased accumulation of β-catenin–myc (compared to control lane 2 [Fig. 3 and Table 1]), but not α-spectrin detected on the same nitrocellulose blot. Microinjection of increasing amounts of *N/C XS6KIIA* mRNA along with *XS6KIIA* mRNA antagonizes this effect (compare lane 4 with decreasing signals in lane 5 and then lane 6). This experiment was repeated three times with comparable results in each case.

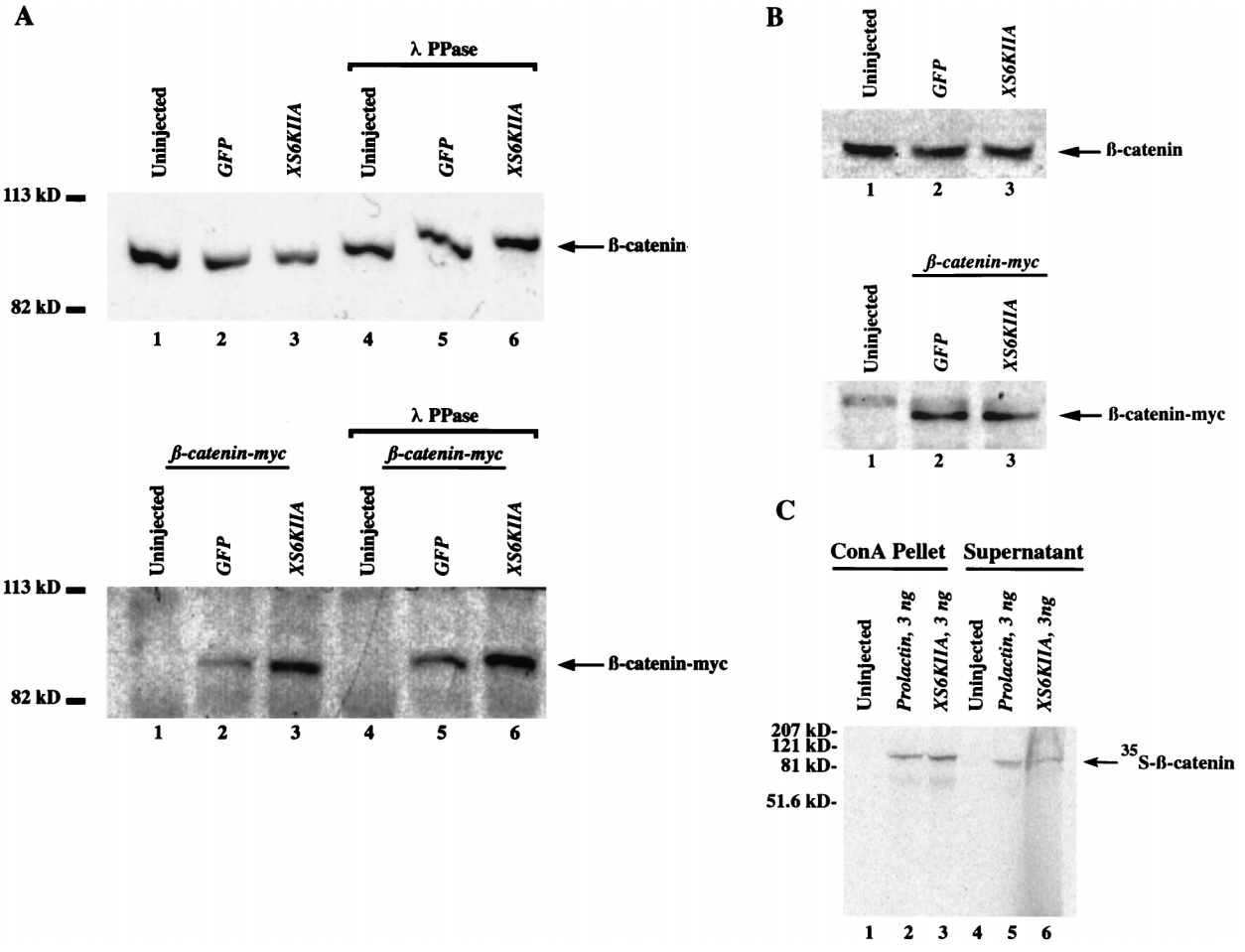


FIG. 5. Overexpression of p90$^{rsk}$ increases the amount of membrane-associated β-catenin. (A) *XS6KIIA* mRNA (1.5 ng) encoding p90$^{rsk}$ was microinjected into the marginal zone of both blastomeres of two-cell embryos. β-Catenin–*myc* mRNA (0.1 ng) was microinjected into the marginal zone of a single blastomere at the four-cell stage. Green fluorescent protein (*GFP*) (1.5 ng) and β-galactosidase (1.5 ng) mRNAs were used to control for nonspecific effects and to maintain a constant amount of microinjected mRNA. To determine whether the overexpression of p90$^{rsk}$ alters the amount of β-catenin associated with cadherins, embryonic protein was extracted in RIPA buffer in the presence of 1% Nonidet P-40 0.5% sodium deoxycholate, and 0.1% SDS to extract membrane-associated β-catenin. ConA-Sepharose beads were used to obtain a cadherin-enriched fraction, whose endogenous and exogenous β-catenin content was analyzed by anti-β-catenin (top gel) and anti-c-*myc* Western blotting (bottom gel), respectively. Overexpression of p90$^{rsk}$ leads to an accumulation of exogenous β-catenin–myc (compare lanes 2 and 3 and lanes 5 and 6, bottom gel). This effect also was observed for endogenous β-catenin but only after λ-phosphatase (λ PPase) treatment (compare lanes 5 and 6, top gel). This suggests that the N-terminal epitope detected by the polyclonal anti-β-catenin antibody used to detect endogenous β-catenin is partially masked by phosphorylation after p90$^{rsk}$ overexpression (compare lane 3 to lanes 1 and 2, top gel). This masking effect is not observed when exogenous β-catenin is detected by using the C-terminal anti-c-*myc* antibody (bottom gel). Only trace amounts of β-catenin and β-catenin–myc were detectable by enhanced chemiluminescence in the supernatant fractions of these experiments (data not shown). (B) Overexpression of p90$^{rsk}$ does not lead to an increase in the steady-state levels of free β-catenin. Cytosolic protein from embryos treated as described above was extracted in buffer H in the absence of detergents. Endogenous and exogenous β-catenin were detected by Western blotting with a polyclonal anti-β-catenin antibody and a monoclonal anti-c-*myc* antibody, respectively. Overexpression of p90$^{rsk}$ did not result in increased steady-state levels of endogenous, free (compare *XS6KIIA*-injected lane 3 to control lanes 1 and 2, top gel) or overexpressed, free myc-tagged β-catenin (compare *XS6KIIA*-injected lane 3 to control lane 2, bottom gel). These experiments were repeated three times with identical results in each case. (C) To simultaneously visualize β-catenin present in the cadherin-enriched ConA-Sepharose pellet and supernatant fractions, we repeated our ConA enrichment experiments (A) after microinjection of in vitro-translated [$^{35}$S]β-catenin, followed by microinjection of RNAs. The λ-phosphatase treatment was omitted from these experiments. As expected, microinjection of *XS6KIIA* (3 ng) but not prolactin (3 ng) RNA resulted in increased levels of [$^{35}$S]β-catenin associated with the ConA pellet (compare lanes 2 and 3) and not the supernatant fractions (compare lanes 5 and 6), as monitored by phosphorImager analysis.

membrane, as assayed by its accumulation in the cadherin-enriched ConA pellet (data not shown).

Since p90$^{rsk}$ was previously shown to regulate GSK-3 activity (14, 62, 66) and our data demonstrates that FGF stimulates p90$^{rsk}$ activity, we next tested whether FGF could inhibit endogenous GSK-3 activity during early *Xenopus* development. Embryo extracts were subjected to FPLC Mono-Q fractionation, and GSK-3 activity was assayed in the flowthrough and wash fractions by using a synthetic phosphopeptide, P9CREB (see Materials and Methods). Western blot analysis confirmed the presence of GSK-3 in these fractions (Fig. 7). We found that ectopic eFGF alone decreased peak GSK-3 activity to 48% of control levels on average (Fig. 7, $n = 2$) and that overexpression of eFGF and p90$^{rsk}$ together did not further inhibit endogenous GSK-3 activity, which remained at an average of 52% of control levels (data not shown; $n = 3$). GSK-3 activity was eluted somewhat later when embryos were treated with eFGF compared to untreated controls (Fig. 7). Using specific antibodies against phosphoserine 9 of GSK-3, we found a significant increase in serine 9 phosphorylation in the FGF-treated fractions compared to that in the untreated samples (Fig. 7, compare the bottom two blots [FGF-treated frac-

TABLE 2. Dorsoanterior index scale in UV-irradiated embryos after *XS6KIIA* mRNA microinjection[a]

| mRNA | DAI[a] | Total no. of embryos |
|---|---|---|
| Control UV | 0.61 | 18 |
| *XS6KIIA* | 0.73 | 41 |
| Nonfunctional *XS6KIIA* | 0.68 | 40 |

[a] Fertilized *Xenopus* eggs were ventralized by UV irradiation (2 to 10 min), and then a single ventral-marginal blastomere was microinjected at the 8- to 16-cell stage with *XS6KIIA* (3.5 ng) or nonfunctional *XS6KIIA* (3.5 ng) mRNA containing a nonsense mutation. At stage 37 to 38, embryos were scored according to the dorsoanterior index (DAI) to quantitate the presence of dorsal structures. The average DAI scores from both experimental treatments resembled that obtained from ventralized controls, indicating that neither treatment was able to rescue the dorsal fate in these embryos ($n = 3$).

tions] with the top two blots [control fractions]). Thus, inhibition of GSK-3 by FGF most probably occurs via the phosphorylation of its serine 9 regulatory site.

## DISCUSSION

In these studies, we searched for a maternally provided upstream kinase that regulates GSK-3 in *Xenopus* embryos. In-gel kinase assays revealed a 90-kDa kinase activity with gels polymerized with Crosstide, a substrate peptide derived from the N terminus of GSK-3 which includes the key regulatory phosphorylation site serine 9 (58, 62, 66). We have identified this kinase as p90$^{rsk}$ based on two separate experiments: (i) immunodepletion of p90$^{rsk}$ from cell extracts prior to the in-gel kinase assays abolished the appearance of the 90-kDa kinase activity band, and (ii) FPLC Mono-Q fractionation of *Xenopus* oocyte extracts revealed a Crosstide kinase peak which coeluted with p90$^{rsk}$ based on Western blot analysis. These initial data suggest that p90$^{rsk}$ lies upstream of GSK-3 during early *Xenopus* embryogenesis. Since FGF (3, 38) and MAP kinase (25, 28, 69) signaling overlaps spatially with p90$^{rsk}$ kinase during mesoderm induction and MAP kinase directly activates p90$^{rsk}$ (18, 62, 64), we hypothesized that p90$^{rsk}$ might be a downstream component of the FGF signaling pathway.

Indeed, we show that p90$^{rsk}$ is strongly activated by FGF during early *Xenopus* embryogenesis. We found that ectopic FGF stimulated endogenous p90$^{rsk}$ kinase activity and, conversely, that inhibition of endogenous FGF signaling by overexpressing a dnFGFR (2) decreased ectopic p90$^{rsk}$ activation compared to the overexpression of p90$^{rsk}$ alone. Coexpression of eFGF with p90$^{rsk}$ led to a synergistic increase in p90$^{rsk}$ activity 170-fold above that of untreated control levels and 88-fold above that for eFGF treatment alone. These data strongly support our view that endogenous *Xenopus* p90$^{rsk}$ is activated by endogenous FGF. During early embryogenesis, *Xenopus* FGF signaling via MAP kinase (25, 28, 41, 69) functions in combination with transforming growth factor β signaling to induce mesoderm around the equator of the embryo (9, 10, 41). Moreover, FGF may work with Wnt signaling to specify neural gene expression (43). We propose that activation of the p90$^{rsk}$ pathway might play a role in mesoderm formation and neural patterning downstream of FGF and MAP kinase.

We demonstrate for the first time that FGF signaling leads to the inhibition of endogenous GSK-3 activity via the phosphorylation of the regulatory residue serine 9. The fact that p90$^{rsk}$ was activated by FGF in embryos and was found to be a major Crosstide kinase in oocyte extracts suggests that inhibition of GSK-3 by FGF is mediated by the activation of MAP kinase and p90$^{rsk}$. We cannot, however, exclude the possibility that other kinases are involved in this process, since several have been implicated in the suppression of GSK-3 activity, usually by 50%, in other cell systems. For example, insulin signaling to GSK-3 was shown to be dependent on PI-3 kinase activation and its downstream target PKB/Akt (11, 48). In contrast, inhibition of GSK-3 by Wnt signaling was reported to be independent of the PI-3 kinase and MAP kinase pathways, since it was not sensitive to either wortmannin or MEK inhibitor (PD098059) but was sensitive to PKC inhibitors (8). Epidermal growth factor and phorbol ester were shown to mediate GSK-3 inhibition via activation of the MAP kinase/p90$^{rsk}$ cascade (14, 62). Since overexpression of PKB/Akt did not modulate β-catenin levels (see Results), we consider PKB to be a less likely upstream regulator of GSK-3 in FGF signaling.

It has been suggested that PKC mediates inhibition of GSK-3 by Wnt signaling (8). However, it is important to note that in contrast to FGF, Wnt signaling does not activate MAP kinase during *Xenopus* embryogenesis (66a). Still, PKC could be a downstream target activated by FGF, as reported for culture cells (68) and bone development (5), and PKC has been reported to activate the MAP kinase pathway via Raf activation (60). Therefore, it is difficult for us to rule out PKC as a potential regulator of GSK-3 in FGF signaling, because manipulation of PKC activity either by specific inhibitors or by overexpression of active mutants of PKC may directly affect MAP kinase and subsequently p90$^{rsk}$ activation, making these experiments difficult to interpret. In addition, the use of specific pharmacological inhibitors is not possible in *Xenopus*, because the vitelline membrane and extracellular material of the embryo render the embryo impermeable. As a final caveat, we found that coexpression of ectopic p90$^{rsk}$ along with FGF in *Xenopus* embryos did not result in further inhibition of endogenous GSK-3 compared to that observed with FGF alone. It is possible that FGF-mediated stimulation of endogenous p90$^{rsk}$ is sufficient to inhibit GSK-3 activity maximally in *Xenopus* embryos, so that ectopic p90$^{rsk}$ has no additional inhibitory effect. An alternate explanation is that our GSK-3 activity assay is not sensitive enough to detect subtle increases in GSK-3 inhibition above and beyond what was observed with ectopic FGF.

In contrast to Wnt/Wingless signaling, which mediates GSK-3 inhibition (8), dorsal-axis duplication (13), and the accumulation of free cytosolic β-catenin (42, 70), our studies show that ectopic FGF/p90$^{rsk}$ signaling does not increase free cytoplasmic β-catenin levels or induce dorsal cell fate even though it decreases GSK-3 activity (3, 38) (see Results). Rather, it increases total β-catenin levels by promoting the association of β-catenin with ConA-binding proteins, most probably cadherins (19, 46), which might prevent β-catenin from degradation by the ubiquitination and proteosome pathway. Previous studies with dominant negative constructs (74) and a GSK-3 inhibitor, lithium chloride (39, 42, 61), have correlated GSK-3 inhibition with the accumulation of free β-catenin. Our studies support a model in which inhibition of GSK-3 via FGF is not sufficient to promote the accumulation of free β-catenin and induce dorsal cell fate in *Xenopus* embryos. It is possible that dominant negative GSK-3 competes for downstream targets of GSK-3 that impinge on β-catenin without, or as well as, altering GSK-3 catalytic activity. Thus, only a subset of the mechanisms by which GSK-3 is inhibited via different signaling pathways may result in the stabilization of free β-catenin. More studies are required to investigate this issue.

Although overexpression of p90$^{rsk}$ did not affect the steady-state levels of cytoplasmic, free β-catenin, it did increase total β-catenin levels by promoting the association of β-catenin with ConA-binding proteins in *Xenopus* embryos. Since cadherins

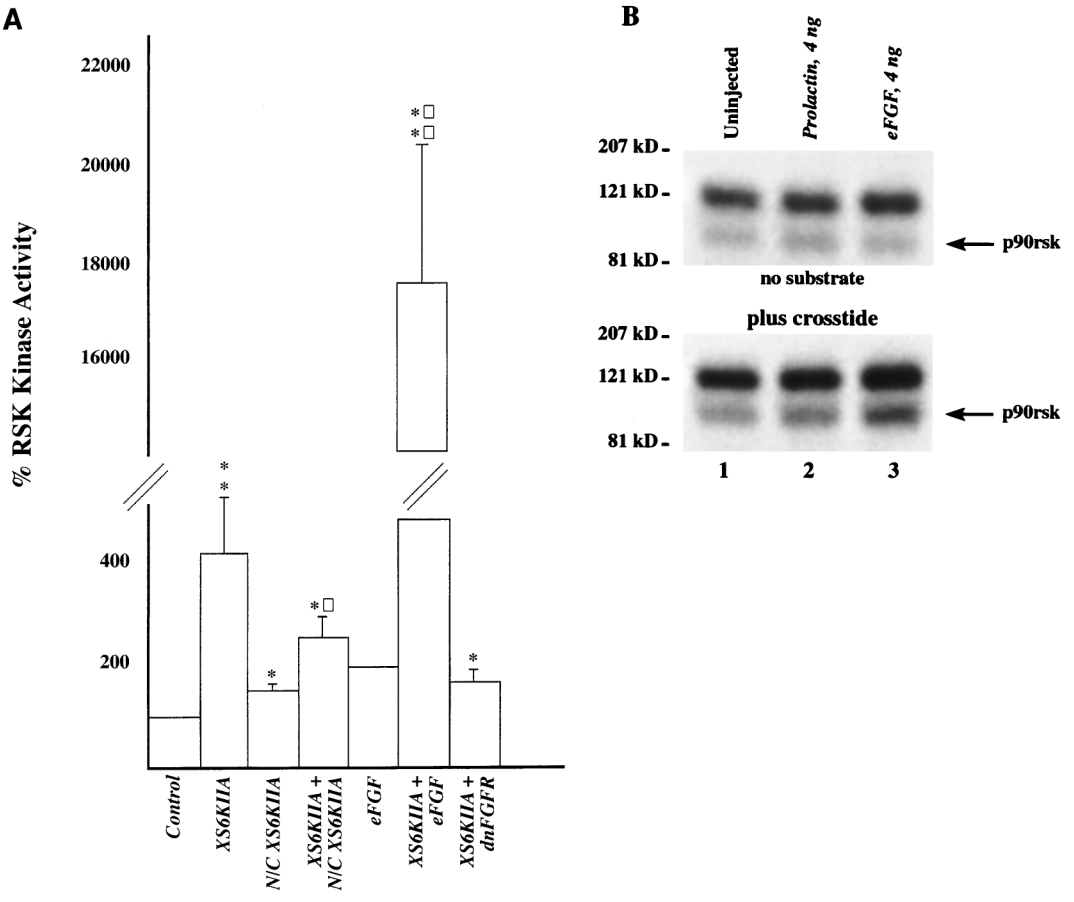


FIG. 6. Overexpression of p90$^{rsk}$ and eFGF leads to increased p90$^{rsk}$ kinase activity in *Xenopus* embryos. (A) *XS6KIIA* (10 ng), *N/C XS6KIIA* (13 ng), eFGF (12 ng), and dnFGFR (6 ng) mRNAs were microinjected alone or in combination into the marginal zone of both blastomeres of two-cell *Xenopus* embryos. Proteins were extracted at stage 8 from 10 to 15 embryos per sample in buffer H in the presence of 1% Triton X-100. p90$^{rsk}$ was immunoprecipitated from these extracts with polyclonal anti-p90$^{rsk}$ antibodies and then incubated with kinase reaction mix, [$\gamma$-$^{32}$P]ATP, and S6 peptide substrate. A 25-$\mu$l sample of the kinase reaction mixture was spotted on p81 paper after 15 min of incubation at 30°C. $^{32}$P incorporation into the S6 peptide substrate is presented. On average, uninjected control p90$^{rsk}$ kinase reactions resulted in a transfer of 106 fmol of [$^{32}$P]phosphate from [$\gamma$-$^{32}$P]ATP to the S6 peptide substrate ($n = 9$). For each experiment, all samples were normalized to control p90$^{rsk}$ kinase activity levels, with controls set at 100% kinase activity. Overexpression of p90$^{rsk}$ by microinjection of *XS6KIIA* mRNA increased p90$^{rsk}$ kinase activity in a statistically significant manner to 414% relative to controls ($P < 0.01$ by Student's $t$ test, $n = 8$). Overexpression of the mutant, putative kinase-dead *N/C* p90$^{rsk}$ by microinjecting *N/C XS6KIIA* mRNA caused a small increase in kinase activity (151%; $P < 0.05$ by Student's $t$ test, $n = 3$). Despite this effect, coinjection of *N/C XS6KIIA* mRNA and *XS6KIIA* mRNA resulted in an inhibition in p90$^{rsk}$ kinase activity from 414 to 251% ($P < 0.02$ by Student's $t$ test, $n = 4$), although this level of kinase activity was still significantly greater than in the controls ($P < 0.05$ by Student's $t$ test, $n = 4$). Microinjection of eFGF mRNA doubled p90$^{rsk}$ kinase activity (200%, $n = 2$), and overexpression of p90$^{rsk}$ and FGF by coinjecting *XS6KIIA* and eFGF mRNA led to a synergistic, statistically significant stimulation of p90$^{rsk}$ kinase activity to 17,717% above control levels ($P < 0.005$ by Student's $t$ test, $n = 4$). This treatment is also significantly greater than the 414% p90$^{rsk}$ activity level obtained by overexpressing p90$^{rsk}$ alone ($P < 0.002$ by Student's $t$ test, $n = 4$). Finally, coinjection of *XS6KIIA* and dnFGFR mRNA to overexpress p90$^{rsk}$ along with a dnFGFR which blocks endogenous FGF signaling led to a 166% level of p90$^{rsk}$ kinase activity relative to controls ($P < 0.05$ by Student's $t$ test, $n = 4$). This level of kinase activity is lower than that obtained from overexpressing p90$^{rsk}$ alone (compare 414% to 166%). Asterisks indicate that the difference in kinase activity relative to controls is statistically significant ($P < 0.05$ for a single asterisk; $P < 0.005$ for a double asterisk). Squares indicate that the difference in kinase activity relative to *XS6KIIA* mRNA treatment is statistically significant ($P < 0.02$ for a single square; $P < 0.002$ for a double square). Error bars represent SE. (B) Microinjection of eFGF (4 ng), but not prolactin (4 ng), mRNA also stimulates p90$^{rsk}$ kinase activity in the in-gel kinase assay, as evident by $^{32}$P incorporation being higher in the p90$^{rsk}$ band in the eFGF-treated samples (lane 3) relative to control samples (lanes 1 and 2) in the presence of Crosstide peptide substrate ($n = 3$ experiments).

are the principal ConA-binding proteins that are able to bind β-catenin (19, 46), it is highly likely that p90$^{rsk}$ increases the amount of β-catenin bound to cadherins in *Xenopus* embryos. Accumulation of cadherin-associated β-catenin in C57MG mammary epithelial cells leads to increased cell-cell adhesion (31), and modulation of cadherin-mediated cell adhesion by overexpression of wild-type cadherins and of dominant negative cadherin constructs leads to inhibited gastrulation movements in *Xenopus* embryos (43, 66a). These data support the hypothesis that a twofold increase in cadherin-associated β-catenin levels might increase cadherin-mediated cell adhesion and consequently alter morphogenetic movements during *Xenopus* embryonic development, consistent with the observed gastrulation-defective p90$^{rsk}$ overexpression phenotype observed in our studies. A phosphatase treatment experiment revealed that ectopic p90$^{rsk}$ increases the N-terminal phosphorylation of the β-catenin associated with ConA-binding proteins. GSK-3 phosphorylation of β-catenin, most probably at the N terminus (74), has been demonstrated to increase the association of β-catenin with cadherins in vitro (46). It is plausible that p90$^{rsk}$-mediated direct or indirect phosphorylation of the N terminus of β-catenin also might increase its association with cadherins, although we do not expect GSK-3 and p90$^{rsk}$ to target the same residues. Other potential mechanisms by which p90$^{rsk}$ might promote the accumulation of β-catenin at the plasma membrane include the modulation of cadherin expression and/or function.

p90$^{rsk}$ was able to increase total β-catenin levels only when

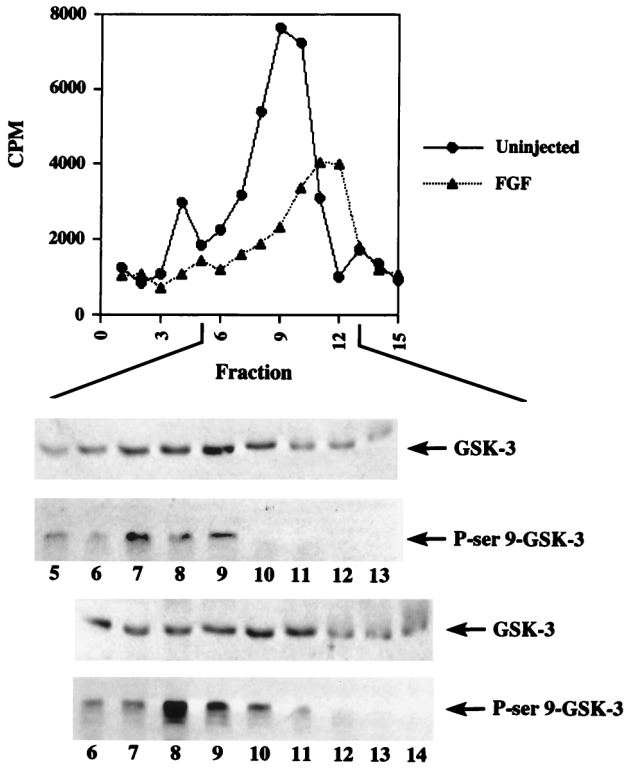


FIG. 7. FGF signaling inhibits endogenous GSK-3 activity. eFGF (10 ng) or eFGF (10 ng) with *XS6KIIA* (10 ng) mRNA was injected into the marginal zone of two-cell *Xenopus* embryos. At embryonic stage 8, proteins were extracted from 50 embryos per sample in modified buffer H with a final Triton X-100 concentration of 0.2%. The samples were then pooled to generate approximately 12 mg of total protein from 450 uninjected or FGF-overexpressing embryos and subjected to FPLC Mono-Q fractionation. Fractions 1 to 5 and 6 to 15 represent the flowthrough and wash fractions, respectively. GSK-3 activity was assayed by incubating fraction aliquots with kinase reaction mix, [$\gamma$-$^{32}$P]ATP, and p9Creb peptide substrate for 15 min at 30°C (see Materials and Methods). The kinase reaction mixtures were then spotted on p81 paper and counted for radioactivity. $^{32}$P incorporation into the p9Creb peptide substrate is presented. On average, peak uninjected control kinase activity resulted in a transfer of 1.2 pmol of [$^{32}$P]phosphate from [$\gamma$-$^{32}$P]ATP to p9Creb peptide ($n$ = 4; 1.5 pmol or 7640 cpm in the experiment shown). This peak correlated with highest level of endogenous GSK-3 protein found in the fractions by Western blot analysis. Overexpression of FGF reduced peak activity to 53% of control levels (4,020 cpm). Again, kinase activity correlated with GSK-3 protein levels (peaks in fraction 9) as determined by Western blotting (top blot). FGF overexpression resulted in the shift of the peak to fraction 11 (third blot from the top). FGF treatment increased GSK-3 serine 9 phosphorylation, as assayed by Western blotting with a monoclonal anti-phosphoserine 9 GSK-3 antibody (compare control fractions [second blot from top] with FGF-treated fractions [bottom blot]). This strongly suggests that FGF signaling inhibits GSK-3 by inducing the phosphorylation of this regulatory residue. The inhibition of GSK-3 activity by microinjection of eFGF and *XS6KIIA* mRNA together (average 52% of control levels, $n$ = 3 experiments) was almost identical to that obtained by overexpression of FGF alone (average 48% of control levels, $n$ = 2). The GSK-3 inhibition shown in this experiment is representative of that observed in all other experiments performed ($n$ = 5). Kinase activity is reported in counts per minute, since equal amounts of total protein were present in the corresponding uninjected and FGF-treated fractions, as determined by the Bradford assay.

overexpressed in the marginal zone of the developing embryo, a region that develops into mesoderm. This result is consistent with a potential role of p90$^{rsk}$ acting downstream of FGF during mesoderm induction. We propose that p90$^{rsk}$ activation by FGF might lead to the redistribution of soluble β-catenin to the plasma membrane during mesoderm development, possibly to alter cadherin-mediated cell adhesion. Since Wnt signaling and FGF signaling can work in a combinatorial manner to induce the dorsal mesoderm (7) and to induce posterior neural tissue (43), it is also possible that coactivation of these pathways intersects through complex regulation of GSK-3 and β-catenin. In summary, our data suggest that p90$^{rsk}$ does not mediate endogenous axis formation but instead identifies p90$^{rsk}$ as a downstream component of FGF signaling and emphasizes that GSK-3 and β-catenin are targets of FGF/p90$^{rsk}$ as well as Wnt signaling during *Xenopus* embryonic development.

## ACKNOWLEDGMENTS

We thank Jonathan Slack for the eFGF cDNA and W. James Nelson for comments on the manuscript.

M.A.T. was an HHMI Predoctoral Fellow, and R.T.M. is an Investigator of the Howard Hughes Medical Institute, which supported this research. H.E.-F. and E.G.K. acknowledge support from National Institutes of Health grant DK-42528.

## REFERENCES

1. **Aberle, H., A. Bauer, J. Stappert, A. Kispert, and R. Kemler.** 1997. β-Catenin is a target for the ubiquitin-proteasome pathway. EMBO J. **16:**3793–3804.
2. **Amaya, E., T. J. Musci, and M. W. Kirschner.** 1991. Expression of a dominant negative mutant of the FGF receptor disrupts mesoderm formation in *Xenopus* embryos. Cell **66:**257–270.
3. **Amaya, E., P. A. Stein, T. J. Musci, and M. W. Kirschner.** 1993. FGF signalling in the early specification of mesoderm in *Xenopus*. Development **118:**477–487.
4. **Bjorbaek, C., Y. Zhao, and D. E. Moller.** 1995. Divergent functional roles for P90rsk kinase domains. J. Biol. Chem. **270:**1–5.
5. **Bradham, D. M., B. Wiesche, P. Precht, R. Balakir, and W. Horton.** 1994. Transrepression of type II collagen by TGF-β and FGF is protein kinase C dependent and is mediated through regulatory sequences in the promoter and first intron. J. Cell. Physiol. **158:**61–68.
6. **Cadigan, K. M., and R. Nusse.** 1997. Wnt signaling: a common theme in animal development. Genes Dev. **11:**3286–3305.
7. **Christian, J. L., D. J. Olson, and R. T. Moon.** 1992. Xwnt-8 modifies the character of mesoderm induced by bFGF in isolated *Xenopus* ectoderm. EMBO J. **11:**33–41.
8. **Cook, D., M. J. Fry, K. Hughes, R. Sumathipala, J. R. Woodgett, and T. C. Dale.** 1996. Wingless inactivates glycogen synthase kinase-3 via an intracellular signalling pathway which involves a protein kinase C. EMBO J. **15:**4526–4536.
9. **Cornell, R. A., and D. Kimelman.** 1994. Activin-mediated mesoderm induction requires FGF. Development **120:**453–462.
10. **Cornell, R. A., T. J. Musci, and D. Kimelman.** 1995. FGF is a prospective competence factor for early activin-type signals in *Xenopus* mesoderm induction. Development **121:**2429–2437.
11. **Cross, D. A. E., D. R. Alessi, P. Cohen, M. Andjelkovich, and B. A. Hemmings.** 1995. Inhibition of glycogen synthase kinase-3 by insulin mediated by protein kinase B. Nature **378:**785–789.
12. **Dominguez, I., K. Itoh, and S. Y. Sokol.** 1995. Role of glycogen synthase kinase 3-β as a negative regulator of dorsoventral axis formation in *Xenopus* embryos. Proc. Natl. Acad. Sci. USA **92:**8498–8502.
13. **Du, S. J., S. Purcell, J. L. Christian, L. L. McGrew, and R. T. Moon.** 1995. Identification of distinct classes and functional domains of *Wnts* through expression of wild-type and chimeric proteins in *Xenopus* embryos. Mol. Cell. Biol. **15:**2625–2634.
14. **Eldar-Finkelman, H., R. Seger, J. R. Vandenheede, and E. G. Krebs.** 1995. Inactivation of glycogen synthase kinase-3 by epidermal growth factor is mediated by mitogen-activated protein kinase/p90 ribosomal protein S6 kinase signaling pathway in NIH/3T3 cells. J. Biol. Chem. **270:**987–990.
15. **Eldar-Finkelman, H., G. M. Argast, O. Foord, E. H. Fischer, and E. G. Krebs.** 1996. Expression and characterization of glycogen synthase kinase-3 mutants and their effect on glycogen synthase activity in intact cells. Proc. Natl. Acad. Sci. USA **93:**10228–10233.
16. **Erikson, E., and J. L. Maller.** 1985. Purification and characterization of a protein kinase from *Xenopus* eggs highly specific for ribosomal protein S6. J. Biol. Chem. **261:**350–355.
17. **Erikson, E., and J. L. Maller.** 1986. A protein kinase from *Xenopus* eggs specific for ribosomal protein S6. Proc. Natl. Acad. Sci. USA **82:**742–746.
18. **Erikson, E., D. Stefanovic, J. Blenis, R. L. Erikson, and J. L. Maller.** 1987. Antibodies to *Xenopus* egg S6 kinase II recognize S6 kinase from progesterone- and insulin-stimulated *Xenopus* oocytes and from proliferating chicken embryo fibroblasts. Mol. Cell. Biol. **7:**3147–3155.
19. **Fagotto, F., N. Funayama, U. Gluck, and B. M. Gumbiner.** 1996. Binding to cadherins antagonizes the signaling activity of beta-catenin during axis formation in *Xenopus*. J. Cell Biol. **132:**1105–1114.
20. **Fisher, T. L., and J. Blenis.** 1996. Evidence for two catalytically active kinase domains in pp90$^{rsk}$. Mol. Cell. Biol. **16:**1212–1219.
21. **Funayama, N., F. Fagotto, P. McCrea, and B. Gumbiner.** 1995. Embryonic

axis induction by the Armadillo repeat domain of β-catenin: evidence for intracellular signaling. J. Cell Biol. **128:**959–968.
22. **Giebelhaus, D. H., B. D. Zelus, S. K. Henchman, and R. T. Moon.** 1987. Changes in the expression of α-fodrin during embryonic development of *Xenopus laevis*. J. Cell Biol. **105:**843–853.
23. **Goode, N., K. Hughes, J. R. Woodgett, and P. J. Parker.** 1992. Differential regulation of glycogen synthase kinase-3β by protein kinase C isotypes. J. Biol. Chem. **267:**16878–16882.
24. **Gotoh, Y., E. Nishida, T. Yamashita, M. Hoshi, M. Kawakami, and H. Sakai.** 1990. Microtubule-associated protein (MAP) kinase activated by nerve growth factor and epidermal growth factor in PC12 cells. Eur. J. Biochem. **193:**661–669.
25. **Gotoh, Y., N. Matsuyama, A. Suzuki, N. Ueno, and E. Nishida.** 1995. Involvement of the MAP kinase cascade in *Xenopus* mesoderm induction. EMBO J. **14:**2491–2498.
26. **Gumbiner, B. M.** 1995. Signal transduction by β-catenin. Curr. Opin. Cell Biol. **7:**634–640.
27. **Gumbiner, B. M.** 1997. Carcinogenesis: a balance between β-catenin and APC. Curr. Biol. **7:**R443–R446.
28. **Hartley, R. S., A. L. Lewellyn, and J. L. Maller.** 1994. MAP kinase is activated during mesoderm induction in *Xenopus laevis*. Dev. Biol. **163:**521–524.
29. **Hayashi, S., B. Rubinfeld, B. Souza, P. Polakis, E. Wieschaus, and A. J. Levine.** 1997. A *Drosophila* homolog of the tumor suppressor gene *adenomatous polyposis coli* downregulates β-catenin by its zygotic expression is not essential for the regulation of armadillo. Proc. Natl. Acad. Sci. USA **94:**242–247.
30. **He, X., J. P. Saint Jaennet, J. R. Woodgett, H. E. Varmus, and I. B. Dawid.** 1995. Glycogen synthase kinase-3 and dorsoventral patterning in *Xenopus* embryos. Nature **374:**617–622.
31. **Hinck, L., W. J. Nelson, and J. Papkoff.** 1994. *Wnt*-1 modulates cell-cell adhesion in mammalian cells by stabilizing β-catenin binding to the cell adhesion protein cadherin. J. Cell Biol. **124:**729–741.
32. **Hoppler, S., J. D. Brown, and R. T. Moon.** 1996. Expression of a dominant negative Wnt blocks induction of MyoD in *Xenopus* embryos. Genes Dev. **10:**2805–2817.
33. **Ikeda, S., S. Kishida, H. Yamamoto, H. Murai, S. Koyama, and A. Kikuchi.** 1998. Axin, a negative regulator of the Wnt signaling pathway, forms a complex with GSK3β and β-catenin and promotes GSK-3β-dependent phosphorylation of β-catenin. EMBO J. **17:**1371–1384.
34. **Isaacs, H. V., M. E. Pownall, and J. M. Slack.** 1994. eFGF regulates *Xbra* expression during *Xenopus* gastrulation. EMBO J. **13:**4469–4481.
35. **Jones, S. W., E. Erikson, J. Blenis, J. L. Maller, and R. L. Erikson.** 1988. A *Xenopus* ribosomal protein S6 kinase has two apparent kinase domains that are each similar to distinct protein kinases. Proc. Natl. Acad. Sci. USA **85:**3377–3381.
36. **Kameshita, I., and H. Fujiawa.** 1989. A sensitive method for detection of calmodulin-dependent protein kinase II activity in sodium dodecyl sulfate-polyacrylamide gel. Anal. Biochem. **183:**139–143.
37. **Kemler, R.** 1993. From cadherins to catenins: cytoplasmic protein interactions and regulation of cell adhesion. Trends Genet. **9:**317–321.
38. **Kimelman, D., J. L. Christian, and R. T. Moon.** 1992. Synergistic principles of development: overlapping patterning systems in *Xenopus* mesoderm induction. Development **116:**1–9.
39. **Klein, P. S., and D. A. Melton.** 1996. A molecular mechanism for the effect of lithium on development. Proc. Natl. Acad. Sci. USA **93:**8455–8459.
40. **Kuehl, M., and D. Wedlich.** 1997. Wnt signaling goes nuclear. Bioessays **19:**229–243.
41. **LaBonne, C., and M. Whitman.** 1994. Mesoderm induction by activin requires FGF-mediated intracellular signals. Development **120:**463–472.
42. **Larabell, C. A., M. Torres, B. A. Rowning, C. Yost, J. R. Miller, M. Wu, D. Kimelman, and R. T. Moon.** 1997. Establishment of the dorso-ventral axis in *Xenopus* embryos is presaged by early asymmetries in β-catenin that are modulated by the Wnt signaling pathway. J. Cell Biol. **136:**1123–1136.
43. **Levine, E., H. Lee, C. Kintner, and B. Gumbiner.** 1994. Selective disruption of E-cadherin function in early *Xenopus* embryos by a dominant negative mutant. Development **120:**901–909.
44. **McGrew, L. L., S. Hoppler, and R. T. Moon.** 1997. Wnt and FGF pathways cooperatively pattern anteroposterior neural ectoderm in *Xenopus*. Mech. Dev. **69:**105–114.
45. **Miller, J. R., and R. T. Moon.** 1996. Signal transduction through β-catenin and specification of cell fate during embryogenesis. Genes Dev. **10:**2527–2539.
46. **Miller, J. R., and R. T. Moon.** 1997. Analysis of the signaling activities of localization mutants of β-catenin during axis specification in *Xenopus*. J. Cell Biol. **139:**229–243.
47. **Morin, P. J., A. B. Sparks, V. Korinek, N. Barker, H. Clevers, B. Vogelstein, and K. W. Kinzler.** 1997. Activation of β-catenin-Tcf signaling in colon cancer by mutations in β-catenin or APC. Science **275:**1787–1790.
48. **Moule, S. K., G. I. Welsh, N. J. Edgell, E. J. Foulstone, C. G. Proud, and R. M. Denton.** 1997. Regulation of protein kinase B and glycogen synthase kinase-3 by insulin and β-adrenergic agonist in rat epididimal fat cells. J. Biol. Chem. **272:**7713–7719.
49. **Munemitsu, S., I. Albert, B. Souza, B. Rubinfeld, and P. Polakis.** 1995. Regulation of intracellular β-catenin levels by the adenomatous poliposis coli (APC) tumor suppressor protein. Proc. Natl. Acad. Sci. USA **92:**3046–3050.
50. **Orford, K., C. Crockett, J. P. Jensen, A. M. Weissman, and S. W. Byers.** 1997. Serine-phosphorylation regulated ubiquitination and degradation of β-catenin. J. Biol. Chem. **272:**24735–24738.
51. **Papkoff, J.** 1997. Regulation of complexed and free catenin pools by distinct mechanisms. Differential effects of *Wnt*-1 and v-*Src*. J. Biol. Chem. **272:**4536–4543.
52. **Pierce, S. B., and D. Kimelman.** 1995. Regulation of Spemann organizer formation by the intracellular kinase *Xgsk-3*. Development **121:**755–765.
53. **Polakis, P.** 1995. Mutations in the APC gene and their implications for protein structure and function. Curr. Opin. Genet. Dev. **5:**66–71.
54. **Rocheleau, C. E., W. D. Downs, R. Liu, C. Wittmann, Y. Bei, Y. H. Cha, M. Ali, J. R. Priess, and C. C. Mello.** 1997. Wnt signaling and an APC-related gene specify endoderm in early *C. elegans* embryos. Cell **90:**707–716.
55. **Rubinfeld, B., B. Souza, I. Albert, O. Muller, S. H. Chamberlain, F. R. Masiarz, S. Munemitsu, and P. Polakis.** 1993. Association of the APC gene product with β-catenin. Science **262:**1731–1734.
56. **Rubinfeld, B., I. Albert, E. Porfiri, C. Fiol, S. Munemitsu, and P. Polakis.** 1996. Binding of the GSK-3β to the APC-β-catenin complex and regulation of complex assembly. Science **272:**1023–1026.
57. **Rubinfeld, B., P. Robbins, M. El-Gamil, I. Albert, E. Porfiri, and P. Polakis.** 1997. Stabilization of β-catenin by genetic defects in melanoma cell lines. Science **275:**1790–1792.
58. **Saito, Y., J. R. Vandenheede, and P. Cohen.** 1994. The mechanism by which epidermal growth factor inhibits glycogen synthase kinase 3 in A431 cells. Biochem. J. **303:**27–31.
59. **Sakanaka, C., J. B. Weiss, and L. T. Williams.** 1998. Bridging of β-catenin and glycogen synthase kinase-3β by Axin and inhibition of β-catenin-mediated transcription. Proc. Natl. Acad. Sci. USA **95:**3020–3023.
60. **Schonwasser, D. C., R. M. Marais, C. J. Marshall, and P. J. Parker.** 1998. Activation of the mitogen-activated protein kinase/extracellular signal-regulated kinase pathway by conventional, novel and atypical protein kinase C isotypes. Mol. Cell. Biol. **18:**790–798.
61. **Stambolic, V., L. Ruel, and J. R. Woodgett.** 1996. Lithium inhibits glycogen synthase kinase-3 activity and mimics wingless signaling in intact cells. Curr. Biol. **6:**1664–1668.
62. **Stambolic, V., and J. R. Woodgett.** 1994. Mitogen inactivation of glycogen synthase kinase-3 beta in intact cells via serine 9 phosphorylation. Biochem. J. **303:**27–31.
63. **Stefanovic, D., E. Erikson, L. J. Pike, and J. L. Maller.** 1986. Activation of a ribosomal protein S6 protein kinase in *Xenopus* oocytes by insulin and insulin-receptor kinases. EMBO J. **5:**1574–1560.
64. **Sturgill, T. W., L. B. Ray, E. Erikson, and J. L. Maller.** 1988. Insulin-stimulated MAP-2 kinase phosphorylates and activates ribosomal protein S6 kinase II. Nature **334:**715–718.
65. **Su, L. K., B. Vogelstein, and K. W. Kinzler.** 1993. Association of the APC tumor suppressor protein with catenins. Science **262:**1734–1737.
66. **Sutherland, C., I. A. Leighton, and P. Cohen.** 1993. Inactivation of glycogen synthase kinase-3β by phosphorylation: new kinase connections in insulin and growth factor signalling. Biochem. J. **296:**15–19.
66a. **Torres, M. A.** Unpublished results.
67. **Torres, M. A., J. A. Yang-Snyder, S. M. Purcell, A. A. DeMarais, L. L. McGrew, and R. T. Moon.** 1996. Activities of the *Wnt*-1 class of secreted signaling factors are antagonized by the *Wnt*-5A class and by a dominant negative cadherin in early *Xenopus* development. J. Cell Biol. **133:**1123–1137.
68. **Tsuda, T., K. Kaibuchi, Y. Kawahara, H. Fukuzaki, and Y. Takai.** 1985. Induction of protein kinase C activation and calcium mobilization by fibroblast growth factor in Swiss 3T3 cells. FEBS Lett. **191:**205–210.
69. **Umbhauer, M., C. J. Marshall, C. S. Mason, R. W. Old, and J. C. Smith.** 1995. Mesoderm induction in *Xenopus* caused by activation of MAP kinase. Nature **376:**58–62.
70. **Van Leeuwen, F., C. H. Samos, and R. Nusse.** 1994. Biological activity of soluble wingless protein in cultured *Drosophila* imaginal disc cells. Nature **368:**342–344.
71. **Vleminckx, K., E. Wong, K. Guger, B. Rubinfeld, P. Polakis, and B. M. Gumbiner.** 1997. Adenomatous poliposis coli tumor suppressor protein has signaling activity in *Xenopus laevis* embryos resulting in the induction of an ectopic dorsoanterior axis. J. Cell Biol. **136:**411–420.
72. **Woodgett, J. R.** 1994. Regulation and functions of the glycogen synthase kinase-3 subfamily. Cancer Biol. **5:**269–275.
73. **Yang-Snyder, J. A., J. R. Miller, J. D. Brown, C.-J. Lai, and R. T. Moon.** 1996. A *frizzled* homolog functions in a vertebrate *Wnt* signaling pathway. Curr. Biol. **6:**1302–1306.
74. **Yost, C., M. Torres, J. R. Miller, E. Huang, D. Kimelman, and R. T. Moon.** 1996. The axis-inducing activity, stability, and subcellular distribution of β-catenin is regulated in *Xenopus* embryos by glycogen synthase kinase-3. Genes Dev. **10:**1443–1454.